

School of Biomedical Engineering
Indian Institute of Technology
(Banaras Hindu University)
Varanasi-221005

CERTIFICATE

It is certified that the work contained in the thesis titled “*Fabrication and Characterization of Thin Film Nanomaterials based Biosensing Devices for Assessing Dynamic Behaviour of Mammalian Cells*” by “*Mr. Uvanesh K.*” has been carried out under our supervision and that this work has not been submitted elsewhere for a degree.

It is further certified that the student has fulfilled all the requirements of Comprehensive Examination, Candidacy and SOTA for the award of Ph.D. Degree.

Weeraj Sharma
30-9-2020

Prof. Neeraj Sharma
(Supervisor)

School of Biomedical Engineering
Indian Institute of Technology
(Banaras Hindu University)
Varanasi - 221005, (U.P.), India.

Sanjeev Kumar Mahto

Dr. Sanjeev Kumar Mahto
(Co-Supervisor)

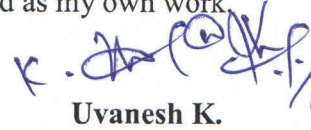
School of Biomedical Engineering
Indian Institute of Technology
(Banaras Hindu University)
Varanasi - 221005, (U.P.), India.

School of Biomedical Engineering
Indian Institute of Technology
(Banaras Hindu University)
Varanasi-221005

DECLARATION BY THE CANDIDATE

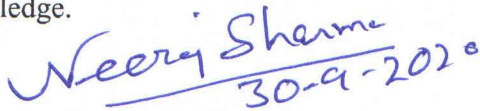
I, *Uvanesh K*, certify that the work embodied in this Ph.D. thesis is my own bonafide work and carried out by me under the supervision of *Prof. Neeraj Sharma* and *Dr. Sanjeev Kumar Mahto* from "21st July 2015" to "30th September 2020" at School of Biomedical Engineering, Indian Institute of Technology (BHU), Varanasi. The matter embodied in this thesis has not been submitted for the award of any other degree/diploma. I declare that I have faithfully acknowledged and given credit to the research workers wherever their works have been cited in my work in this thesis. I further declare that, I have not willfully copied any other's work, paragraphs, text, data, results, etc. reported in the journals, books, magazines, reports, dissertations, theses, etc., or available at websites and have not included them in this Ph.D. thesis and have not cited as my own work.

Date: 29/9/2020
Place: IIT (BHU), Varanasi

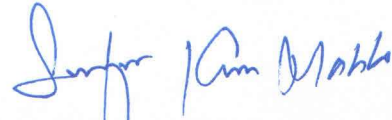

Uvanesh K.

CERTIFICATE BY THE SUPERVISOR(S)

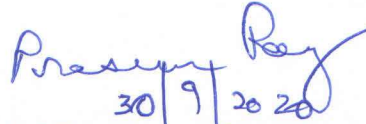
It is certified that the above statement made by the student is correct to the best of our knowledge.


30-9-2020

Prof. Neeraj Sharma
(Supervisor)



Dr. Sanjeev Kumar Mahto
(Co-Supervisor)


30/9/2020

Signature of Head of Department/Coordinator of School
"SEAL OF THE DEPARTMENT/SCHOOL"

समन्वयक/CO-ORDINATOR
जैव चिकित्सा अभियांत्रिकी स्कूल
SCHOOL OF BIOMEDICAL ENGG.
भारतीय प्रौद्योगिकी संस्थान (का.हि.वि.)
INDIAN INSTITUTE OF TECHNOLOGY (B.H.U.)
वाराणसी-221005/VARANASI-221005

School of Biomedical Engineering
Indian Institute of Technology
(Banaras Hindu University)
Varanasi-221005

COPYRIGHT TRANSFER CERTIFICATE

Title of the Thesis : Fabrication and Characterization of Thin Film Nanomaterials based Biosensing Devices for Assessing Dynamic Behaviour of Mammalian Cells

Candidate's Name : Mr. Uvanesh K.

Copyright Transfer

The undersigned hereby assigns to the Indian Institute of Technology (Banaras Hindu University) Varanasi all rights under copyright that may exist in and for the above thesis submitted for the award of the "*DOCTOR OF PHILOSOPHY*".

Date: 29/9/2020

Place: Varanasi



Uvanesh K.

Note: However, the author may reproduce or authorize others to reproduce material extracted verbatim from the thesis or derivative of the thesis for author's personal use provided that the source and University's copyright notice are indicated.

ACKNOWLEDGEMENTS

Foremost, I would like to express my sincerest regards and love for **my father Shri Kasiviswanathan, mother Smt. Jayanthi, and wife Smt. Niveditha** for their constant support and love throughout my life. I will always be in debt no matter what I do, and I will always be your reflection. They are the source of strength for me and remain an invaluable asset to me.

Besides my parents, I would like to express my immense gratitude to my supervisors **Prof. Neeraj Sharma** and **Dr. Sanjeev Kumar Mahto** for their excellent guidance and motivation. The completion of this research work is indeed an outcome of their constant untiring support, valuable ideas, and suggestions during my research work. The insightful discussions with them always provided me great enthusiasm.

I wish to express my immense gratitude to **Prof. Satyabrata Jit**, Department of Electronics Engineering for his constant untiring support to work in the CRME laboratory in order to perform my research work.

I wish to extend my sincere gratitude towards my research performance evaluation committee (RPEC) members: **Dr. Shiru Sharma**, SBME and **Prof. S. K. Singh**, Department of Computer Science and Engineering for their encouragement and insightful comments.

I am grateful to my M. Tech. supervisor **Dr. Kunal Pal**, NIT Rourkela for enlightening me for the further research.

I gratefully acknowledge **Prof. P. K. Roy**, Coordinator, and **Dr. S. K. Rai**, DPGC Convener of the school for the smoothful processing of all official documents. I would like to sincerely thank all the supporting staff of the School for their kind help whenever I required.

I would also like to thank all the faculty members: **Dr. K. Jeyakumar**, Department of Chemistry, and **Dr. V. Ganesan**, Department of Chemistry, BHU for their help and encouragement during this journey.

I am grateful to **Ministry of Human Resources and Development**, Government of India for providing financial assistance in the form of Teaching Assistantship (TA) and contingency to carry out the research work.

I am grateful to **SRISTI organization** for selecting my thesis work for the prestigious SITARE-BIRAC-Gandhian Young Technological Innovation (GYTI) Award 2019, and BIRAC, Government of India for providing financial assistance to carry out the research work.

I would like to express my special thanks to **Dr. Balavigneswaran, Dr. Chandan Kumar**, and **Mr. Amit Kumar** their valuable assistance from personal to the technical level.

I would like to thank my seniors **Dr. Vijay Kumar M.R., Dr. S. Satheesh Kumar, Dr. Nishant Singh, Dr. Chandan Kumar Choubey, Dr. Munendra Singh, Dr. Gaurav Kumar, Dr. Kiran Yellappa**, and **Dr. Sumedha Mukarjee** for sharing their fruitful knowledge and experience.

I would also like to thank all my friends, batchmates, and juniors: **Mr. G. Gopichand, Mr. Alok Prakash, Mrs. Devyani Shukla, Mr. Romel Bhattacharjee, Mr. Ajay Kumar Sahi, Dr. Suruchi Poddar, Mr. Sumit Tripathi, Mr. Taresh Shavesh Sharan, Mr. Chiranjeev Sagar, Mr. Alok Tiwari**, and all for providing a fun-filled environment.

I would like to thank **Dr. Hemant Kumar, Dr. Yogesh Kumar Mr. Abhinav Pratap Singh, Mr. Rishibrind Kumar Upadhyay, Mr. Deep Chandra Upadhyay**, and all for their extended support while working at CRME lab, Department of Electronics Engineering.

My thanks and sincere appreciations also go to all staff members of CRME laboratory for their kind co-operation.

Finally, My most profound appreciation towards **my sister (Preethika)** for her unconditional love, extreme patience and constant support over the years.

Above all, I thank Lord Shiva & Parvathy for providing me strength and courage in completing the work.

Date : 29/09/2020

Place : Varanasi



(Uvanesh K.)

Dedicated
To
My Family

Table of Contents

S. No.	Description	Page No.
a)	List of Figures	xi
b)	List of Tables	xvi
c)	List of Abbreviations	xvii
d)	List of Symbols	xx
e)	Preface	xxiii
1.0	Chapter 1: Introduction	1
1.1	Biosensor	1
1.2	Cell-based biosensor	3
1.3	Classification of cell-based biosensor	5
1.3.1	Electrochemical biosensor for CBB	5
1.3.1.1	Amperometric biosensor	6
1.3.1.2	Potentiometric biosensor	7
1.3.1.3	Impedimetric biosensor	11
1.3.2	Optical biosensor	15
1.3.2.1	Surface plasma resonance (SPR)	16
1.3.2.2	Resonant waveguide grating (RWG)	17
1.3.2.3	Luminescence-based optical chemical sensing (OCS)	18
1.3.3	Piezoelectric biosensor	19
1.4	Strategies for the design and characterization of CBB	20
1.4.1	Design for fabricating the CBB	21
1.4.1.1	Choice of sensing material	21
1.4.1.2	Structure for fabricating the CBB	22
1.4.1.3	Thin film deposition techniques for fabricating the CBB	23
1.4.2	Classification techniques for the fabricated CBB	24
1.4.3	Fundamental behavior of the electric field	25
1.5	Literature review	28
1.5.1	Review on ECIS systems for CBB	29
1.5.2	Review on thin film based electronic devices for CBB	30
1.5.3	Major observation from the literature survey	31

1.6	Research objectives	32
1.7	Scope of the thesis	33
2.0	Chapter 2: Low-cost Electric Cell–Substrate Impedance Sensing System	35
2.1	Outline	35
2.2	Materials and methods	36
2.2.1	Material	36
2.2.2	Microelectrode design and fabrication	37
2.2.3	Cell culture procedure	37
2.2.4	Voltage controlled constant current source (VCCS) unit construction and testing	38
2.2.5	Equivalent electrical circuit Model for the cell-electrode interface	41
2.2.6	Complete Electric Cell-substrate Impedance Sensing (ECIS) system	41
2.3	Results and discussion	46
2.4	Conclusion	59
3.0	Chapter 3: Aluminium Oxide Thin-Film based Biosensing Device	60
3.1	Outline	60
3.2	Materials and methods	61
3.2.1	Materials	61
3.2.2	Fabrication of MIM biosensor	62
3.2.3	Cell culture procedure	63
3.3	Results and discussion	63
3.4	Conclusion	70
4.0	Chapter 4: Zinc oxide coated Metal-Semiconductor-Metal based Biosensing Device	71
4.1	Outline	71
4.2	Materials and methods	72
4.2.1	Materials	72
4.2.2	Sol-gel synthesis of ZnO	72
4.2.3	Sensor fabricated process	72
4.2.4	Cell culture procedure	74
4.3	Results and discussion	75

4.3.1	Thin film characterization of spin coated ZnO device	75
4.3.2	Surface modification of ZnO thin film	80
4.3.2.1	Fourier Transform Infrared (FT-IR) spectroscopic study	82
4.3.2.2	Cell viability and proliferation	84
4.3.3	Electrical characterisation of fabricated cell MSM device	85
4.3.4	Optical and electrical characterisation of fabricated gelatin-GA-APTES-cell MSM device	87
4.3.4.1	Case 1-1000 cells/well concentration	87
4.3.4.2	Case 2-5000 cells/well concentration	90
4.4	Conclusion	92
5.0	Chapter 5: Extended Large Area Heterojunction Biosensing Device	94
5.1	Outline	94
5.2	Experimental details	96
5.2.1	Sensor fabrication procedure	96
5.2.2	Primary cortical neuron cell culture procedure	97
5.2.3	Surface modification	98
5.2.4	Fluorescent staining of nuclei and actin cytoskeleton of neuronal cells	99
5.3	Results and discussion	99
5.3.1	Electrical characterisation of fabricated extended larger area heterojunction device	100
5.3.2	Optical and electrical characterisation of fabricated cell culture attached extended larger area heterojunction device	102
5.4	Conclusion	106
6.0	Chapter 6: Summary and future scope	107
6.1	Summary	107
6.2	Future scope	110
	References	111
	Author's Relevant Publications	140

List of figures

Figure No.	Description	Page No.
1.1	Illustration of biosensor.	1
1.2	The biosensor concept proposed by L.C Clark.	2
1.3	Cell-based biosensing device and zoomed images showing the influence of various stimuli namely chemical, biological, and physical on the cells to cause cellular functions and the changes is being converted into a measurable electric signal by the transducer element. The image is adapted from [21] with some modifications.	4
1.4	Electrodes of electrochemical biosensor (a) two-electrode system, and (b) three-electrode system.	5
1.5	Types of potentiometric sensors used (a) ISFET, (b) EIS capacitive sensor, and (c) LAPS devices.	8
1.6	EnFET's structure with its principle of operation.	9
1.7	Bio-impedance technique based on the type; (a) active, and (b) passive type bio-impedance. (re-used with slight modifications with permission from Springer Nature copyright [43]).	12
1.8	ECIS system having a pair of co-planar electrode, signal generator, current limiting resistor, and lock-in amplifier.	14
1.9	Adherent cells growing on an electrode system with its corresponding change in impedance value due to progression of cellular functions; where (1) when no cells is inoculated; an increase in the impedance value is due to (2) cells starts to adhere on the surface, (3) cellular proliferation, (4) cell-cell interaction on the surface; and decrease in the impedance value due to (5) loss of tight junction or adhesion or cell membrane integrity.	14
1.10	Surface plasmon resonance (SPR) in Kretschmann configuration for CBB.	17
1.11	Resonant waveguide grating (RWG) for CBB.	18

1.12	Luminescence-based OCS for CBB.	19
1.13	Quartz crystal microbalance (QCM) for CBB.	20
1.14	Types of co-planar electrode arrangement used; (a) Interdigitated electrode (IDE), and (b)-(e) dissimilar & similar-sized electrodes.	22
1.15	Sol-gel spin coating process	24
1.16	(a) Thermal, and (b) Electron beam vacuum deposition method.	24
1.17	(a) A schematic diagram of an inverted fluorescence microscope, and (b) Pictograph of the semiconductor parameter analyser (SPA).	25
1.18	Biological cells in electric field, while (a) cell placed in an electric field., (b) cell membrane is represented by as a capacitor due to its hydrophobic nature, (c) adherent cells grown on a conducting surface (metal).	27
2.1	(a) Microelectrode design pattern used; (b) Customized cell-culture chamber developed.	37
2.2	Calibration graph using different R_1 values.	40
2.3	(a) Actual ECIS system, and (b) Constructed experimental (wireless) setup used with 2.5 kHz exciting frequency.	42
2.4	Schematic pictorial representation of the developed device.	43
2.5	Flowchart for calculating the impedance; (a) Transmitting end, and (b) Receiving end.	45
2.6	Morphological changes of C2C12 cells at various time point. (a) 3 h, (b) 6 h, (c) 18 h, (d) 32 h, (e) 48 h, and (f) 72 h; Scale bar: 20 μm .	46
2.7	Change in cell proliferation with respect to average magnitude of impedance over the calibrated area. (a) Frequency vs. Magnitude (b) Frequency vs. Phase (c) Nyquist plot shows the change in semi-circle diameter due to the change in transfer of electrons between the metal-electrode interface resistances.	48

2.8	Rate of proliferation with respect to impedance (a) Normalized impedance vs. frequency plot, and (b) Time point vs. change in impedance and average cell count per image.	49
2.9	Morphology of the C2C12 cells present near the electrode (a) 6 h, (b) 18 h, (c) 36 h, (d) 48 h, and (e) 72 h; Scale bar: 20 μm .	51
2.10	Equivalent circuit model of biological cells (a) Fricke-Morse model, (c) modified Fricke-Morse model, (d) Cole-Cole model, and (f) modified Cole-Cole model. While (b & e) are simplification step.	52
2.11	Shows the experimental data and its fitting.	55
3.1	Fabrication process of EBE deposition Al_2O_3 thin film based biosensing device.	63
3.2	Morphology of C2C12 cells at various time intervals: (a) 8 h, (b) 24 h, (c) 48 h, and (d) 72 h; Scale bar: 50 μm .	64
3.3	Changes in the characteristic electrical properties of the Al_2O_3 thin film due to dynamic behaviour of myoblast cells in culture: (a) capacitance vs. frequency plot, (b) magnitude of impedance plot, (c) phase of impedance plot, (d) Nyquist plot and (e) Average cell count at different time point.	66
3.4	Equivalent electrical circuit model to represent the surface-electrode-cell interface: (a) fabricated device component, (b) tissue component, (c) fabricated device with tissue component and (d) cell-device.	68
4.1	ZnO sol-gel preparation method and its spin coating process.	73
4.2	Transparent ZnO thin film coated MSM based biosensor fabrication process.	74
4.3	(a) XRD pattern of spin coated ZnO thin film, (b) Williamson-Hall (W-H) plot used for calculating average strain (ϵ) and crystallite size.	76
4.4	(a) AFM micrograph, and (b) HR-SEM image of spin coated	77

	ZnO thin film.	
4.5	(a) Absorbance spectra, and (b) Tauc's plot of spin coated ZnO thin film.	79
4.6	EDX pattern of spin coated ZnO thin film with elemental composition table.	79
4.7	Schematic illustration of gelatin functionalization on spin coated ZnO thin film.	81
4.8	FT-IR spectra of pristine gelatin, surface unmodified ZnO thin film and surface modified ZnO thin film.	83
4.9	Cell viability and proliferation of C2C12 cells using MTT assay.	85
4.10	(a) $I-V$ characteristics of fabricated and simulated MSM device (b) Band diagram for the device structure.	86
4.11	Morphological changes of C2C12 cells at various time: (a) 6 h, (b) 24 h, (c) 48 h, (d) 72 h, (e) 96 h, and (f) 120 h; Scale bar: 20 μm .	88
4.12	Electrical properties of the ZnO thin film with respect to change in cell proliferation (1000 cells seeded): (a) $I-V$ characteristics plot, (b) Capacitance vs. frequency plot, (c) Magnitude of impedance plot, (d) Phase of impedance plot, (e) Nyquist plot, and (f) Time vs. change in impedance and average cell count plot.	89
4.13	Morphological changes of C2C12 cells at various time: (a) 24 h, (b) 48 h, (c) 72 h, (d) 96 h, (e) 120 h, (f) 144 h, (g) 168 h, and (h) 210 h ; Scale bar: 20 μm .	91
4.14	Electrical properties of the ZnO thin film with respect to change in cell proliferation (5000 cells seeded): (a) $I-V$ characteristics plot, (b) Capacitance vs. frequency plot, (c) Magnitude of impedance plot, (d) Phase of impedance plot, (e) Nyquist plot, and (f) Time vs. change in impedance and average cell count plot.	92
5.1	An extended larger area heterojunction device with cell	98

	culture well fabrication process.	
5.2	(a) Energy band diagram for the Si/ZnO heterojunction structure, (b) C-V characteristics of the fabricated Si/ZnO heterojunction, and (c) $I-V$ characteristics of fabricated and simulated Si/ZnO heterojunction.	101
5.3	Change in electrical (resistance, conductive) properties of the spin coated ZnO thin film with respect to change in various cell functionality. (a) $I-V$ characteristics plot; (b) Magnitude of impedance plot; (c) Phase of impedance plot; and (d) Nyquist plot.	103
5.4	Fluorescent image shows morphological changes of cortical neuronal cells (a-c) Day 3, and (d-f) Day 5 ; Scale bar: 20 μm .	105
5.5	SEM image shows morphological changes of cortical neuronal cells (a) Day 3, and (b) Day 5.	105
5.6	Micrograph shows morphological changes of cortical neuronal cells at various time point (a) Day 1, (b) Day 3, and, (c) Day 5.	106

List of Tables

Table No.	Description	Page No.
2.1	Cost comparison of the device in USD	44
2.2	Analytical values through an equivalent electrical circuit model of adherent cell-electrolyte-electrode system (Fitting data derived from best of five developed microelectrode system).	57
3.1	Calculated EEC model parameters.	70
4.1	Calculated XRD parameters.	76
4.2	Calculated AFM parameters.	78
4.3	Parameters used for the simulation of ITO/ZnO/ITO device.	86
5.1	Parameters used for the simulation of Al/Si/ZnO/Al heterojunction.	101

LIST OF ABBREVIATIONS

Abbreviation	Details
CBA	Cell-based assay
CBB	Cell-based biosensor
FETs	Field-effect transistors
MOSFET	Metal oxide semiconductor field-effect transistor
MISFET	Metal-insulator-semiconductor field-effect transistor
ECIS	Electric cell-substrate impedance sensing
CO ₂	Carbon dioxide
OP-AMP IC	Operational amplifier integrated circuit
DMEM	Dulbecco's Modified Eagle's Medium high glucose
PBS	Phosphate buffered saline
FBS	Fetal bovine serum
CMOS	Complementary metal-oxide-semiconductor
RF	Radio frequency
VCCS	Voltage controlled constant current source
EEC	Equivalent electrical circuit model
DAQ	Data Acquisition
DSO	Digital storage oscilloscope
CPE	Constant phase element
MIM	Metal-insulator-metal
AFM	Atomic force microscopy
SEM	Scanning electron microscopy
EDX or EDS	Energy dispersive X-ray spectroscopy
XRD	X-ray diffraction
FTIR	Fourier transform infrared spectroscopy
UV- <i>Vis</i>	Ultraviolet-visible
MSM	Metal-semiconductor-metal

MOS	Metal-oxide-semiconductor
SPA	Semiconductor parameter analyser
SMU	Source and measuring unit
MIS	Metal-insulator-semiconductor
ZnO	Zinc oxide
Au	Gold
Ag	Silver
Al	Aluminum
ITO	Indium-doped tin oxide
Si	Silicon
Al ₂ O ₃	Aluminum Oxide
HCl	Hydrochloric acid
EBE	Electron beam evaporation unit
PDMS	Polydimethylsiloxane
APTES	(3-Aminopropyl)-triethoxysilane
GA	Glutaraldehyde solution
MEA	Monoethanolamine
PVDF	Polyvinylidene difluoride
MTT assay	3-(4, 5 dimethylthiazol-2)-2, 5-diphenyltetrazolium bromide
DMSO	Dimethyl sulfoxide
DAPI	4,6-diamidino-2-phenylindole
BSA	Bovine serum albumin
PLL	Poly-L-lysine
FWHM	Full width half maxima
IDE	Interdigital electrode
rms	Root mean square
sccm	Standard cubic centimeters per minute
KCl	Potassium chloride

Na ⁺	Sodium ion
K ⁺	Potassium ion
Ca ²⁺	Calcium ion
Cl ⁻	Chloride ion
H ⁺	Hydrogen ion
O ₂	Oxygen
H ₂ O	Water
Cd ²⁺	Cadmium ion
Cu ²⁺	Cupric ion
Hg ²⁺	Mercuric cation
Pb ²⁺	Lead ion
WE	Working electrode
RE	Reference electrode
pH	potential of hydrogen
EMG	Electromyography
EOG	Electrooculography
ECG	Electrocardiogram
EEG	Electroencephalogram
IS	Impedance spectroscopy
ECL	Electrochemiluminescence
RI	Refractive index
DIC	Digital interference contrast microscopy
SPR	Surface plasmon resonance
RWG	Resonant waveguide grating
OCS	Optical chemical sensing
RA	Resonance angle
QCM	Quartz crystal microbalance
SAW	surface acoustic wave

LIST OF SYMBOLS

Symbol	Details
λ	Wavelength
θ	Diffraction angle
T	Transmittance
A	Absorbance
$I-V$	Current-voltage
$C-V$	Capacitance-voltage
W	Channel width
L	Channel length
e	Charge of electron
C	Cell membrane
X_C, Q	Reactance
R_1, R, R_f	Resistance
Z	Total impedance
C_{dl}	Double layered capacitance
R_{dl}	Double layered resistance
α, n	Dimensionless exponent parameter
R^2	Correlation coefficient
Z_{re}	True or real impedance
R_0	Lower frequency component resistance
R_∞	Higher frequency component resistance
R_i	Intracellular resistance
R_e	Extracellular resistance
M	Mole

h	Hour
min	Minute
s	Second
°C	degree Celsius
RT	Room Temperature
mm	Millimeter
nm	Nanometer
rpm	Revolutions per minute
ϵ	strain
W	watt
V	volt
g	Gram
μg	Microgram
μL	Microliter
mL	Milliliter
Ω	Ohm
k Ω	Kilo Ohm
M Ω	Mega Ohm
Hz	Hertz
kHz	Kilohertz
MHz	Megahertz
ϕ	Phase
R _m	Membrane resistance
C _m	Membrane capacitance
μ	Micro

I	current
\$	United states dollar (USD)
A	Ampere
μA	Microampere
F	farads
\vec{E}	Electric field
I_D	drain current
I_{DS}	Source-drain current
V_G	Gate potential
V_{P-P}	Peak - peak voltage
%	Percentage
\AA	Angstrom
wt.	weight

Biosensor is an analytical device that consists of a biological component to detect an analyte, coupled with a physical transducer to produce a measurable signal. Biosensors have been widely explored and extensively utilized as a platform for applications in pharmaceutical, environment, food and medical field. Amongst the various classes of biosensors developed so far, cell-based biosensors express promising potential in comprehending fundamental biological processes with reference to a whole cell or a group of cells. The direct use of living cells offers exceptional opportunities for bio-detection and drug discovery. The biochemical effect of the direct spatial contact of living cells is converted into quantitative electrical signals by sensors or transducers, thus bridging the gap between electronics and biology. Cell-based biosensors are endowed with certain advantages in comparison to molecule-based approaches for example, noninvasive long-term recordings, label-free detection, reduced response time, etc. In order to achieve the objectives, the thesis has been divided into following chapters.

Chapter-1 introduces the basics about biosensor and cell-based biosensor; Types of cell-based biosensor currently being used. Different types of cell-based biosensor based on its transduction principle; Strategies for the Design and Characterization of CBB and fundamental behaviour of cells in electric field. Literature review and the observation; Research objective and scope of the present study.

Chapter-2 describes the investigation of functional behaviour of myoblast (C2C12) cells using a co-planar silver metal electrode system integrated to a low-cost ECIS system. Typically, the silver metal was thermally coated on the conversional glass substrate to construct metal-insulator-metal (MIM) structure *via* shadow mask method, to achieve an active layer's dimensions of 1.5 mm wide and 4 mm length. At the same time, to develop

a ECIS system, we used the electronic components available at the laboratory to construct a low-cost impedance measuring circuitry and calibrated the developed circuit, against the standard commercial resistor. Further, the MIM device was integrated to the developed impedance measuring circuitry to construct a low-cost ECIS system. To increase the cell adhesion process, the MIM device was coated with 2% gelatin protein and the gelatin-coated MIM device was used as a platform to study the phenotypic change of adherent mammalian cells under the influence of applied electric field. Further, the fabricated biosensor was electrically and optically characterised to validate the outcome.

Chapter 3 focuses on fabrication and characterization of metal-oxide thin film nanomaterials based biosensing devices for assessing dynamic behaviour of adherent mammalian cells. Typically, the Chapter 3 investigates the effect induced by cellular functional behaviour on the characteristic electrical properties of the e-beam deposited aluminium oxide (Al_2O_3) thin film nanomaterial-based metal-insulator-metal (MIM) device. A patterned indium tin oxide (ITO) coated glass substrate having a co-planar electrode dimension of $12 \times 5 \text{ mm}^2$ at each side with a gap of $1 \pm 0.2 \text{ mm}$ (at center) was used as a transparent electrode system. To fabricate the MIM device, Al_2O_3 thin film of $\sim 100 \text{ nm}$ thickness was deposited on ITO electrode system and used as the active sensing interface. To increase the cell adhesion process, the MIM device was coated with 2% gelatin protein and the gelatin-coated MIM device was used as a platform to study the phenotypic change of adherent mammalian cells under the influence of applied electric field. Further, the fabricated biosensor was electrically and optically characterised to validate the outcome.

Chapter 4 investigates the effect induced by cellular functional behaviour on the characteristic electrical properties of the sol-gel synthesized spin coated zinc oxide (ZnO) thin film nanomaterial-based metal-semiconductor-metal (MSM) device. A patterned

indium tin oxide (ITO) coated glass substrate having a co-planar electrode dimension of $12 \times 5 \text{ mm}^2$ at each side with a gap of $1 \pm 0.2 \text{ mm}$ (at center) was used as a transparent electrode system. To fabricate the MSM device, ZnO thin film of $\sim 100 \text{ nm}$ thickness was deposited on ITO electrode system and used as the active sensing interface. To increase the cell adhesion process, the MSM device was coated with 2% gelatin protein and the gelatin-coated MIM device was used as a platform to study the phenotypic change of adherent mammalian cells under the influence of applied electric field. Further, the fabricated biosensor was electrically and optically characterised to validate the outcome.

Chapter 5 investigates the effect induced by cellular functional behaviour on the characteristic electrical properties of the sol-gel synthesized spin coated zinc oxide (ZnO) thin film nanomaterial-based larger area heterojunction device. To fabricate the larger area heterojunction device, ZnO thin film of $\sim 200 \text{ nm}$ thickness was deposited p-type Si substrate, and to create ohmic contact, the aluminium metal electrode was used on both p-Si and n-ZnO. While, ZnO was used as the active sensing interface. To increase the cell adhesion process, the fabricated heterojunction device was functionalized with poly-L-lysine and the poly-L-lysine functionalized ZnO thin film based extended larger area heterojunction device was further characterized for assessing the cell-induced electrical characteristic property change.

Finally, **Chapter 6** summarizes the major objectives and concludes the major findings of the present thesis. This chapter also outlines some future scope of works related to this thesis.